

BEAM DYNAMICS STUDY AND ELECTRODYNAMICS SIMULATIONS FOR THE CW RFQ

S. Polozov^{1,2}, W. Barth^{1,3,4}, T. Kulevoy^{1,2}, Yu. Lozeev¹, S. Yarymyshev^{1,3}

¹ National Research Nuclear University - Moscow Engineering Physics Institute, Moscow, Russia

² Institute for Theoretical and Experimental Physics of NRC Kurchatov Institute, Moscow, Russia

³ GSI Helmholtzzentrum für Schwerionenforschung, Darmstadt, Germany

⁴ HIM Helmholtz-Institut Mainz, Germany

Abstract

A compact "university scale" CW research proton accelerator, as well as a driver linac with three branches of experimental beam lines, delivering beam energy of 3, 30 and 100 MeV for experiments, are recently under development in Russia. The recently developed advanced RFQ cavity design is presented. The results of beam dynamics simulations are discussed.

INTRODUCTION

The development of CW high-power proton linacs is a very actual aim of linear accelerator technology developments. Such a linac is useful for large scale research complexes as SNS or ADS. Also compact low or medium-energy linacs (usually called university class facilities) can be used for several applications as boron-neutron capture therapy (BNCT), high productivity isotopes generation and material science [1, 2].

GSI, MEPhI and ITEP of NRC Kurchatov Institute have a wide experience of high current heavy ion linac development and construction for compact research facilities, as well as for large accelerator complexes [3-16]. Recently the new 2 MeV CW RFQ is under common investigation [17-19]. R&D of CW applications is important step in an RFQ development. The maximum beam current was fixed to 10 mA; the operating frequency has been set to 162 MHz; the RF potential should be limited by 1.3-1.5 of Kilpatrick criterion for CW mode [20, 21]. The main RFQ parameters are shown in Table 1.

Table 1: Main Parameters of the CW RFQ

Ions	protons
Input energy	46 keV
Output energy	2.0 MeV
Frequency	162 MHz
Voltage	90 kV
Length	345 cm
Average radius	0.530 cm
Vanes half-width	0.412 cm
Modulation	1.000 - 2.250
Synchr. phase	-90° - -33°
Max. input beam current	10 mA
Max. input beam emittance	6 cm·mrad (total)
Particle transmission	> 99%

Beam dynamics simulations for the new RFQ channel, as well as an analysis of the RFQ characteristics, have been performed with the codes BEAMDULAC [22] and

DYNAMION [23], providing for a cross-check of the design features and the calculated results. The results of the beam dynamics simulations have been discussed in [18-19]. Further beam dynamics optimization and the first results of the the four-vane RFQ cavity design are presented and discussed in this paper.

BEAM DYNAMICS SIMULATIONS RESULTS AND OPTIMIZATION

The shape of the RFQ input radial matcher has been optimized for a smooth matching of the beam emittance to the RFQ acceptance. The matched Twiss-parameters have been obtained from the results of dedicated simulations for the RFQ acceptance. The same 6D phase space input macroparticle distribution (2σ truncated Gaussian in transverse phase planes and continuous in longitudinal one) has been introduced into both codes for beam dynamics simulations with low beam current.

The resulted particle distributions behind the RFQ (Fig. 1) demonstrate good coincidence between the codes BEAMDULAC and DYNAMION.

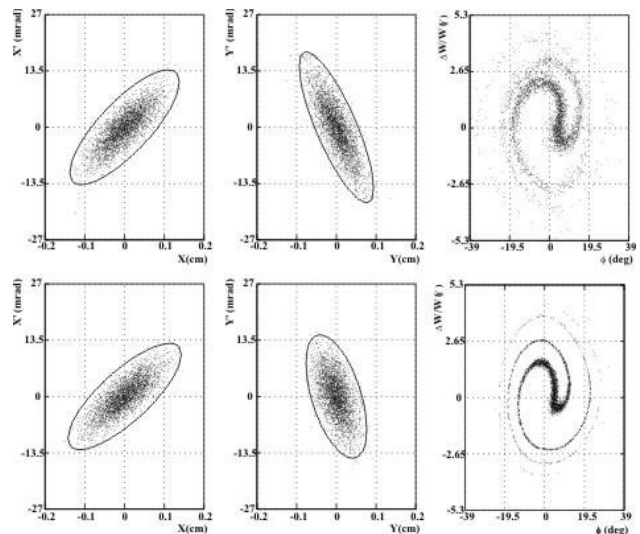


Figure 1: The beam phase portraits behind RFQ for transverse and longitudinal phase planes, simulated by the codes BEAMDULAC (top) and DYNAMION (bottom); ellipses represent 99% of the particles.

Beam brilliance at some position inside a linac could be analysed by means of a dedicated procedure, which calculates the RMS and total beam emittances for a given macroparticle ensemble, and cut some fixed amount of the

most outer particles. Then the procedure is implemented to the rest of the macroparticles, iteratively down to 50% level of the full beam intensity [12].

The developed algorithm has been used for a detailed comparison of the results of beam dynamics simulations, performed by means of the codes BEAMDULAC and DYNAMION.

The beam brilliance analysis for the vertical phase plane behind the RFQ is presented in Fig. 2 and demonstrates a good coincidence between two codes. The results for the horizontal and longitudinal phase planes are at the same level of consistency (Fig. 2).

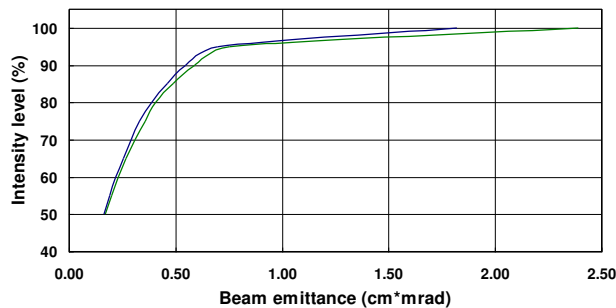


Figure 2: Beam intensity inside a given total beam emittance behind the RFQ channel, calculated from the results of the codes BEAMDULAC (green) and DYNAMION (blue).

Also a set of simulations under space charge conditions, even taking into account low tune depression of a few percent only, is recently under consideration together with the final optimization of the modulation and synchronous phase along the RFQ accelerating-focusing channel.

CW RFQ CAVITY DESIGN AND SIMULATION

The four-vane RFQ cavity with coupling windows [24] can be utilized as a front-end for a high-energy high-power linac. A segmented four-vane RFQ type (SVRFQ), successfully commissioned in 2016 for the new NICA injector at JINR (Dubna) [7, 25-27], was also proposed to be used for CW application [17].

The four-vane cavity of 345 cm length comprises thirteen regular resonant cells and two end cells. The length of the resonant cell is $L_{cell}=22.6$ cm. The 3D model of the RFQ cavity is shown in Fig. 3. Such structure was tuned to the operating frequency of 162 MHz by means of the magnetic coupling windows optimization. Note that coupling windows on vertical vanes are shifted by $L_{cell}/2$ from horizontal vanes.

The TE_{211} quadrupole mode is the ground one for the recent RFQ cavity design. The electrical and the magnetic field dislocation are strongly separated. The electrical field is concentrated in the near-axis area (Fig. 4a), while the magnetic field is located in the quadrants (Fig. 4b). Obviously the operating quadrupole mode is effectively tuned.

ISBN 978-3-95450-182-3

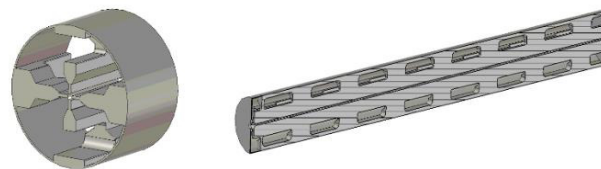


Figure 3: 3D model of the segmented four-vane RFQ cavity with coupling windows.

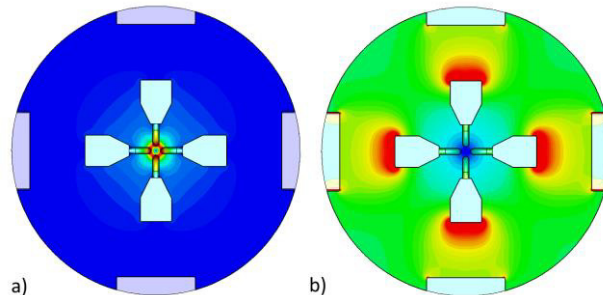


Figure 4: Cavity transverse cut: electrical (a) and magnetic (b) field distribution.

The high order modes, close to the operating one, were studied additionally. The dipole mode TE_{111} occurred to be the nearest to the ground one. It was suggested to increase both transverse and longitudinal size of the magnetic coupling windows to separate the dipole mode from the quadrupole one. After optimization the frequency shift between the two modes is about 7 MHz.

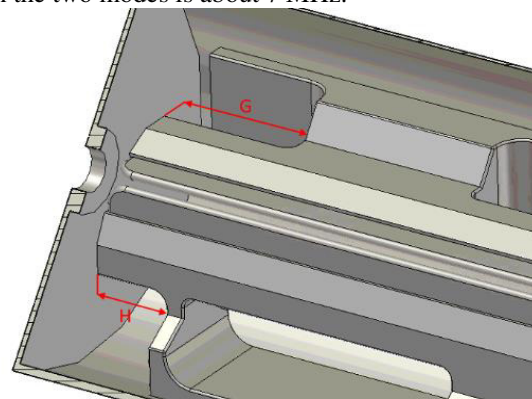


Figure 5: The model of the end region of the SVRFQ cavity with the boss on the end cup and an additional window (with length of H) on the end pole.

The tuning of the RF field distribution along the cavity axis should be performed to minimize a nonlinearity. The size of gaps between vanes and end caps determine the field drops in gaps and also introduce the nonlinearity along of vanes. The field amplitude on end cap gaps should be tuned to be close to the values inside the regular part of the cavity. Such parameters of the cavity's end cells, as length and height of the end coupling windows, as well as length, diameter and thickness of the boss placed on caps, and the distance between the boss and vanes (see Fig. 5) can be used to tune the RF field distribution at the end of the cavity. Additionally a small window can be also added to the end pole.

04 Hadron Accelerators

A08 Linear Accelerators

For this study a length of the end coupling widows is used as a parameter to tune the RF field distribution. The length of the regular half-window G as well as the length of the additional window on the end pole H were varied in a wide range to optimize the RF field amplitude distribution. The minimum irregularity of the field distribution of about 2.5% has been achieved with $H=7$ cm and $G=13$ cm (Fig. 6).

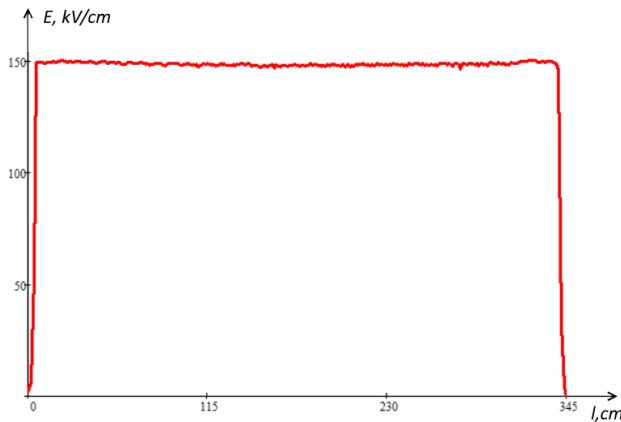


Figure 6: Distribution of electrical field along the cavity axis; the maximum nonlinearity is limited by 2.5%.

It should be noted, that during optimization of the cavity geometry and RF field amplitude the resonant frequency decreases by 3 MHz. Therefore the size of windows or the cavity radius should be reduced to compensate such a perturbation.

As long as reduction of windows size causes the weakening of quadrupole and dipole mode separation, the frequency was tuned by means of decreasing of the cavity radius. The geometrical parameters for the cavity and electrodynamic characteristics after optimization are given in Table 2.

Table 2: Geometrical Characteristics for the Optimal SVRFQ Design and Main Electrodynamic Characteristics

Parameter	Value
Frequency, MHz	162.0
Shell radius R_{shell} , mm	183.0
Transverse window length, $\%R_{shell}$	49.0
Conjugate window length, $\%L_{cell}$	122.0
1 st end region length, $\%L_{cell}$	113.0
2 nd end region length, $\%L_{cell}$	113.0
Power losses, kW	220
Q-factor	9540
Transverse shunt impedance, k Ω	13.0
RF field amplitude distribution nonlinearity, %	<2.5

ACKNOWLEDGEMENT

This project is supported in part by the MEPhI 5/100 Program of the Russian Academic Excellence Project.

CONCLUSION

A new CW 2 MeV RFQ linac is now under development by the common MEPhI and ITEP team. The maximum field strength is limited by the 1.5 Kilpatrick criterion to provide for the stable cw operation. The proposed RFQ linac can accelerate a 10 mA proton beam with a particle transmission close to 100%. The codes BEAM-DULAC and DYNAMION have been used for beam dynamics simulations. Current results of the RFQ channel optimization are presented. The segmented four-vane cavity (SVRFQ) is proposed to use for such RFQ. The results of the electrodynamic parameter study demonstrate high performance of the SVRFQ cavity.

REFERENCES

- [1] C.R. Prior, Proc. of HB'10, 6-10 (2010).
- [2] L. Weissman et al., Journal of Instrumentation, 10, T1004 (2015).
- [3] S.M. Polozov et al., Proc. of HB'2016, 188-190 (2016).
- [4] W. Barth et al., Proc. of Baldin ISHEPP XXIII (2016), EPJ Web of Conferences 138, 01026 (2017).
- [5] A.E. Aksentyev, P.N. Alekseev, K.A. Aliev et al., Atomic Energy, 117, Issue 4, 270-277 (2015).
- [6] A.E. Aksentyev et al., Atomic Energy, 117, Issue 5, 347-356 (2015).
- [7] V.A. Andreev, A.I. Balabin, A.V. Butenko et al., Prob. of Atomic Sci. and Tech., 6 (88), 8-12 (2013).
- [8] W. Barth, W. Bayer, L. Dahl et al., NIM A, 577, Issues 1-2, 211-214 (2007).
- [9] W. Barth et al., PRST AB 18(4), 040101 (2015).
- [10] F. Herfurth et al., Physica Scripta, T166 (T166):014065 (2015).
- [11] W. Barth et al., Phys. Rev. ST Accel. Beams 18(5), 050102 (2015)
- [12] S. Yaramyshev et al., Phys. Rev. ST Accel. Beams 18(5), 050103 (2015)
- [13] W. Barth et al., Proc. of IPAC'2016, 2052-2054 (2016), Phys. Rev. ST Accel. Beams (in press).
- [14] W. Barth et al., Proc. of HB'2016, 319-322 (2016).
- [15] S. Yaramyshev et al., Proc. of HB'2016, 751-754 (2016).
- [16] F. Dziuba et al., Proc. of RuPAC'16, 83-85 (2016).
- [17] A.E. Aksentyev, T. Kulevoy, S.M. Polozov, Proc. of IPAC'14, 3286-3288 (2014).
- [18] S.M. Polozov et al., Proc. of HB'2016, 188-190 (2016).
- [19] S.M. Polozov et al., Proc. of RuPAC'16, 267-269 (2016).
- [20] I.M. Kapchinsky, "About approximations of Kilpatrick criterion", PTE №1, 33-35 (1986).
- [21] I.M. Kapchinsky, "Theory of linear resonance accelerators", Moscow, (1982).
- [22] S.M. Polozov, Prob. of Atomic Sci. and Tech., 3(79), 131-136 (2012).
- [23] S. Yaramyshev et al., NIM A, 558/1, 90-94 (2006).
- [24] V.A. Andreev, Patent US5483130 (1996).

- [25] V. Aleksandrov et al., Proc. of IPAC'16, 941-943 (2016).
- [26] S.M. Polozov et al., Proc. of RuPAC'16, 267-269 (2016).
- [27] A.V. Butenko et al. Proc. of RuPAC'16, 153-155 (2016).